

The role of particle size of glyburide crystals in improving its oral absorption

Yongjun Wang¹ · Wenqian Yang¹ · Qiang Fu¹ · Zhibin Guo¹ · Bingjun Sun¹ · Wen Liu¹ · Yaxuan Liu¹ · Simeng Mu¹ · Mengran Guo¹ · Jingru Li¹ · Xiaohui Pu¹ · Zhonggui He¹

Published online: 31 March 2017
© Controlled Release Society 2017

Abstract Currently, nanosizing is becoming increasingly prevalent as an efficient way for the improvement of oral drug absorption. This study mainly focuses on two points, namely the crystal properties, and the in vitro and in vivo characterizations of drug crystals during the nanosizing process. We used glyburide, an oral type 2 diabetes (T2D) medication, as our model drug. We sought to reduce the crystalline size of this drug and evaluate its absorption properties by comparing it with the original coarse drug because of previous reports about its gastrointestinal absorption insufficiency. Glyburide crystals, ranging from 237.6 to 4473 nm were prepared successfully by jet milling and media milling. The particle sizes and the crystal morphology were analyzed by characterization of the solid states, equilibrium solubility, and dissolution behavior. Additionally, pharmacokinetic study was performed in SD rats. The solid state results indicated a loss in crystallinity, amide-imidic acid interconversion, and partial amorphization during nanosizing. Further, in in vitro tests, nanocrystal formulations remarkably increased the solubility and dissolution of the drug (compared to microcrystals). In the in vivo test, reducing the particle size from 601.3 to 312.5 nm showed no improvement on the C_{\max} and $AUC_{(0-36\text{ h})}$ values, while a profound slowing of the drug elimination occurred with reduction of particle size. Further reduction from 312.5 to 237.6 nm lead to a significant increase ($p < 0.001$) of the $AUC_{(0-36\text{ h})}$ from $6857.8 \pm 369.3\text{ ng mL}^{-1}\text{ h}$ to $12,928.3 \pm 1591.4\text{ ng mL}^{-1}\text{ h}$, respectively, in rats. Our

present study confirmed that nanosizing has a tremendous impact on promoting the oral absorption of glyburide.

Keywords Nanosizing · Glyburide · Nanocrystal · Crystalline · Oral bioavailability

Introduction

There has been an expansion in the use of active pharmaceutical ingredients in the last two decades due to the advances in high-throughput screening and combinatorial chemistry. Unfortunately, about 70–90% of these active compounds have absorption issues, with poor aqueous solubility [1]. Poor solubility, characterized by some oral administered drugs, poses a problem, in that it restricts their biopharmaceutics and pharmacokinetic properties and subsequently, their pharmaceutical efficiency. A way to overcome this major obstacle commonly faced by formulation scientists is to improve the solubility of such drugs by using formulation strategies [2–4]. A well-established and relatively simple approach used to solve this problem is particle size reduction [5].

As predicted by the Ostwald–Freundlich and Kelvin equations, the saturation solubility of a drug is dependent on its particle size and particle curvature [6]; and the Noyes–Whitney equation has been used to correlate a drug particle size with its dissolution rate [7]. Reduction of drug particle size effectively increases its surface area, decreases thickness of the diffusion layer, and enhances solubility. These effects can dramatically improve the dissolution rate and simultaneously increase oral bioavailability [3]. Furthermore, various studies have demonstrated nanosize optimizations, enable achievement of smaller particle size, and consequently, improve bioavailability [8–10].

✉ Yongjun Wang
i_maple@163.com

¹ Shenyang Pharmaceutical University, Shenyang, People's Republic of China

In general, top-down (breaking up large particles into smaller ones), bottom-up (building up nanoparticles from molecules) techniques, and combined approaches are often used for nanosizing [8, 11]. Typically, the top-down approaches mainly involve homogenization or milling while the bottom-up approaches, primarily are based on the principle of precipitation [12]. In the process of formulation design, aspects such as stabilizers selection, homogenization/milling time, pressure, speed, and milling media are often discussed in the literature [13–15]. In these reports, nanosizing was used to show poorly water soluble drugs can be absorbed and ensured delivery to target sites. To fully understand the in vivo fate of nanocrystals, our previous work further demonstrated different in vitro and in vivo performances of rod-shaped and spherical-shaped lovastatin nanocrystals [16] and the relationship between dissolution and pharmacokinetics for nimodipine nanocrystals [17]. There remain certain aspects, however, that needed careful investigation. Different drug crystals required different production time to achieve a particular minimal particle size. Whether the crystalline transformation and amorphization will occur by the high energy input during the nanosizing process remain to be elucidated. Additionally, no systematical study has described the influence of the nanosizing process on the crystal properties. Thus, the crystal state during nanosizing process requires careful analysis.

Our present study focused on two main points, crystals properties, and the in vitro and in vivo characterizations of drug crystals during the nanosizing process. Glyburide, the model drug, is among the Class II drugs in the biopharmaceutical classification system [18]. In this study, glyburide microcrystals and three nanocrystals ranging from 4.4 μm to 263.6 nm were prepared from the microcrystals by jet milling and media milling. During the nanosizing process, the drug crystal properties needed to be defined. We used the following techniques to characterize glyburide nanosizing: (1) dynamic light scattering; (2) scanning electron microscopy (SEM); (3) transmission electron microscopy (TEM); (4) differential scanning calorimetry (DSC); (5) powder X-ray diffractometry (PXRD); (6) Fourier-transform infrared spectroscopy (FT-IR); and (7) Raman spectroscopy (Raman). Finally, in vitro dissolution and in vivo pharmacokinetic studies were conducted, which revealed a positive correlation between glyburide nanosizing and oral intestinal absorption.

Materials and methods

Materials

Glyburide was purchased from the Tianjin Institute of Pharmaceutical Research Co., Ltd. (Tianjin, China). Polyvinylpyrrolidone K30 (PVP K30) and Lutrol poloxamer

407 (F127) were a gift by BASF Co., Ltd. (Shanghai, China). Hydroxypropyl methylcellulose E5 (HPMC-E5) was obtained from Anhui Sunhere Pharmaceutical Excipients Co., Ltd. (Huainan, China). Sodium dodecyl sulfate (SDS) and sucrose were obtained from Tianjin Bodi Chemical Holding Co., Ltd. (Tianjin, China). Methanol (HPLC grade) was supplied by Tianjin Kemer Chemical Reagent Co., Ltd. (Tianjin, China). N-hexane and dichloromethane were obtained from Concord Technology Co., Ltd. (Tianjin, China).

Preparation of glyburide formulations

Preparation of glyburide microcrystals

Glyburide microcrystals were prepared using an RT-25 jet milling machine (Beijing Yanshan Zhengde Machinery Equipment Co., Ltd., Beijing, China). Glyburide coarse powder was added into a powder feeder and then freshly micronized. The injector pressure and grinding pressure were kept at 0.6 and 0.4 MPa, respectively. The mill was maintained at a feeding rate of 1 g/min, using compressed air as the carrier.

Preparation of glyburide nanocrystals

Glyburide coarse powder and stabilizer were added into a beaker and mixed using magnetic stirring, followed by media milling with a BBX24B Bullet Blender Blue homogenizer (Next Advance, Inc., USA). These two procedures were conducted to generate homogeneous suspension. Further, 1 mL of zirconium dioxide beads were added to 1 mL of the suspension. Subsequently, nanocrystals with different particle sizes were obtained by changing the stabilizer and varying the milling parameters, as shown in Table 1.

Freeze-drying

Characterization and pharmacokinetic studies were carried out to improve the physical stability of glyburide nanocrystals, which was further used for physicochemical analysis. The procedures used were as follows: Samples were lyophilized using an FDU-1100 EYELA freeze dryer (Tokyo Rikakikai Co., Ltd., Tokyo, Japan), and sucrose (5%, w/v) was used as the cryoprotective agent. Initially, samples were frozen at

Table 1 Nanocrystal stabilizer and milling parameters

	Stabilizers	Milling time (min)	Bead diameters (mm)
Nano-1	PVPK30 (6%, w/v)	25	0.1
Nano-2	PVPK30 (6%, w/v)	12	0.5
Nano-3	PVPK30 (6%, w/v)	9	0.5

–80 °C for 8 h. Then a two-step cold drying was performed at –40 °C for 3 h, followed by –20 °C for 15 h. Finally, a one-step mild temperature drying was performed at 30 °C for 3 h.

Characterization of nanocrystals

Particle size

The particle sizes and polydispersity indexes (PDI) of the nanocrystals were determined using a Zetasizer Nano ZS90 instrument (Malvern Instruments Ltd., Malvern, UK). All samples were diluted 500-fold and measured at 25 °C at a scattering angle of 90°. Each sample was measured in triplicate for 14 cycles. Microcrystals were measured using a Mastersizer 3000 instrument (Malvern Instruments Ltd., Malvern, UK). The dispersion pressure was kept at 2 bars, with a feed rate range of 50%.

SEM

The morphologies of the raw crystals microcrystals and nanocrystals were examined using an SU8010 field emission SEM (Hitachi Ltd., Tokyo, Japan), to identify particles with a better resolution. Samples were coated with a thin layer of gold and placed on conductive double-sided carbon tapes. The accelerating voltage mode used to collect secondary electrons emitted by the atoms of the drug crystals was 20 kV.

TEM

To further confirm the morphology and shape of the glyburide nanocrystals, samples were examined using a JEM-2100, TEM (JEOL Ltd., Tokyo, Japan). Briefly, 10 µL of diluted nanocrystals (0.5 mg/mL) was dropped on copper grids with a 200-mesh carbon supported membrane and dried at room temperature. Then, 2% phosphotungstic acid solution was added for 30 s to stain the nanocrystals. After drying in the air for 10 s, the samples were observed at an accelerating voltage of 200 kV.

DSC

DSC analysis was conducted using a DSC 1 instrument (Mettler-Toledo International Inc., Schwerzenbach, Switzerland). The thermal properties of the coarse glyburide, its microcrystals, physical mixture, and its nanocrystals were analyzed. For DSC measurement, each sample was weighed accurately in pierced aluminum pans and heated at a 10 °C/min rate, from 25 to 200 °C in a nitrogen atmosphere. Aluminum oxide was used as a reference in all of the studies.

PXRD

We analyzed the crystallinity of the coarse drug, microcrystals, and nanocrystals, by using a D/Max 2500 PC X-ray diffractometer (Rigaku Corporation, Tokyo, Japan) over a 2θ range of 3° to 50° at a scanning rate of 1°/min. We operated the equipment at a voltage of 40 kV and a current of 40 mA. Moreover, a vertical goniometer was used to measure the scattered radiation.

FT-IR

The interaction between drug and excipients was analyzed using an FT-IR spectrometer (Bruker Corporation, Switzerland) at room temperature. The samples were compressed into small pellets with potassium bromide (KBr) scanned over the range 4000 to 400 cm⁻¹.

Raman spectroscopy

Raman spectroscopy was conducted to analyze crystal samples with rough uneven or curved surfaces, using a Renishaw InVia Raman microscope (Gloucestershire, UK) which was equipped with a 532 nm laser. The laser power was 100 mW and the integration time was 10 s.

In vitro evaluation

Equilibrium solubility measurement

We added excess glyburide (about 6 mg) to 10 mL tubes ($n = 3$) containing 9 mL distilled water. The tubes were shaken continuously in a water bath maintained at 37 °C. At 1, 4, 8, 24, 48, and 72 h, the equilibrated samples were passed through a 0.22 µm membrane filter (Tianjin Kemer Chemical Reagent Co., Ltd., China) and 1 mL of each filtrate was diluted with equal volume of methanol. Finally, the amount of dissolved drug was analyzed quantitatively for each sample by HPLC.

In vitro dissolution test

We used ZRS-8G dissolution tester (Tianjin Tianda Tianfa Technology Co., Ltd., Tianjin, China) to evaluate the in vitro dissolution performance of glyburide crystals. (Paddle method, Electrolab Dissolution Tester TDT-06P, USP). Powder samples of the coarse drug, microcrystals, and nanocrystals (equivalent to 2.5 mg glyburide) were dispersed in 250 mL phosphate buffer solution (pH 6.8 ± 0.05) containing 0.3% SDS. The tests were conducted at 37 °C with a paddle speed of 75 rpm. At 0.25, 0.5, 1, 2, 3, and 4 h, samples (10 mL each) were withdrawn and replaced with the same volume of fresh medium. Then, each sample was passed through a 0.22 µm membrane filter. Each filtrate was then diluted with methanol

and quantitatively analyzed by high-performance liquid chromatography (HPLC).

HPLC analysis

HPLC technique was used to evaluate the drug contents employing a Waters e2695 HPLC system, consisting of a 2489 UV/Visible Detector and a 515 pump (Waters Technology Co., Ltd., Shanghai, China). The drug concentrations were analyzed using a validated HPLC method [19]. An ODS Cosmosil 5C18-AR-II column (150 mm × 4.6 mm, 4.5 μm) with UV detection at 300 nm was used as a mixture of ammonium dihydrogen phosphate (pH 3.5) / methanol at 37.5:62.5, as the eluent at a flow rate of 1.0 ml/min. The concentration of each sample was calculated by the external standard method with a glyburide retention time (RT) 10.9 min.

Pharmacokinetic study

Animal studies

The protocols for our animal studies were approved by the Animal Ethics Committee of Shenyang Pharmaceutical University (Shenyang, China). Animal experiments were performed according to the “Guidelines for the Care and Use of Laboratory Animals.” Male Sprague-Dawley (SD) rats weighing 250 ± 20 g were randomly assigned to five groups ($n = 6$). The rats fasted for 12 h before the study, and all groups were administered with a single oral dose of 10 mg glyburide. Blood samples (0.3 mL) were collected from the suborbital venous plexus and transferred to heparinized tubes at 0.17, 0.5, 1, 2, 3, 4, 6, 8, 12, 24, 36, and 48 h. After centrifugation at 13,000 rpm for 10 min, a plasma sample was obtained at each time point, for each group and stored at -20 °C until required for LC-MS-MS analysis.

Plasma processing

Glyburide was extracted using a liquid-liquid extraction procedure. For sample preparation, 20 μL of an internal standard solution (250 ng/mL, glipizide) and 20 μL of initial mobile phase were added to 100 μL plasma samples. Afterward, 50 μL phosphoric acid (0.25 M) and 3 mL extraction solvent (n-hexane: dichloromethane at a volume ratio of 1:1) were added, mixed for 3 min, and then centrifuged at 3500 rpm for 10 min. The organic layer obtained was transferred to a clean vial and evaporated at 40 °C under a gentle nitrogen purge. Dried residue was re-dissolved in 100 μL mobile phase and centrifuged at 15,000 rpm for 10 min. Finally, 5 μL of supernatant from each sample was injected into the LC-MS-MS system.

LC-MS-MS analysis

An ACQUITY UPLC™ system (Waters Co., Ltd., Milford, MA, USA) was used to determine the plasma drug concentration, using a validated LC-MS-MS method [20]. The separation was performed using an ACQUITY UPLC BEH C18 column (50 mm × 2.1 mm, 1.7 μm; Waters Co., Ltd., Milford, MA, USA) and quantification was executed using multiple transition reaction monitoring of the m/z 446 → 321 for glipizide and m/z 494 → 369 for glyburide, respectively. The standard curve was linear ($r^2 > 0.99$) over the range 1–3000 ng/mL. The lower limit of quantification was 1 ng/mL.

Statistical analysis

The results of the analysis were expressed as mean ± S.E. One-way ANOVA was carried out using IBM SPSS Statistics 21 software. Differences were considered statistically significant if the p value was less than or equal to 0.05.

Results and discussion

Formulation and preparation of drug crystals

The results of our present studies show that jet milling and media milling are capable of breaking up coarse glyburide into the micron and nano range. In this process, factors such as the size of the milling media, type, and a number of stabilizers, milling speed and time, were optimized to obtain the desired particle size and polydispersity index (PdI). Then, nanocrystals were freeze-dried to improve their physical stability for further characterization: Sucrose (5% w/v) was added to each formulation to prevent crystal agglomeration and ensure complete redispersion. The dry powders obtained were loose and dispersible. We evaluated the apparent particle size of the nanocrystals and microcrystals, using dynamic light scattering and laser diffraction. The results are shown in Table 2. After micronization, the d_{50} (which means that 50% of the particles by volume are smaller than the given value) of the microcrystals was reduced to 4.473 μm. Nanocrystals were prepared using media milling, exhibited a relatively low PdI, suggesting that the drug crystals were uniform.

Morphology

The SEM and TEM micrographs in Fig. 1 show changes in the crystal size reduction process. The particle sizes shown in the pictures are consistent with the above-measured diameters. Microcrystals (Fig. 1) aggregated into small particles with no uniform size and shape. Compared with microcrystals,

Table 2 Particle size and Pdl of glyburide (data are expressed as mean \pm S.D., $n = 3$)

Preparation	Before freeze-drying		After freeze-drying	
	Mean diameter (nm)	PdI	Mean diameter (nm)	PdI
Microcrystals	4437	–	–	–
Nano-3	601.3 \pm 21.85	0.347 \pm 0.042	681.3 \pm 15.81	0.429 \pm 0.220
Nano-2	312.5 \pm 21.83	0.299 \pm 0.041	344.5 \pm 8.194	0.253 \pm 0.034
Nano-1	237.6 \pm 4.788	0.159 \pm 0.028	246.7 \pm 6.512	0.223 \pm 0.028

the nanocrystals (Fig. 1b, c, d) had a relatively uniform size distribution and random morphology.

Crystal characterization

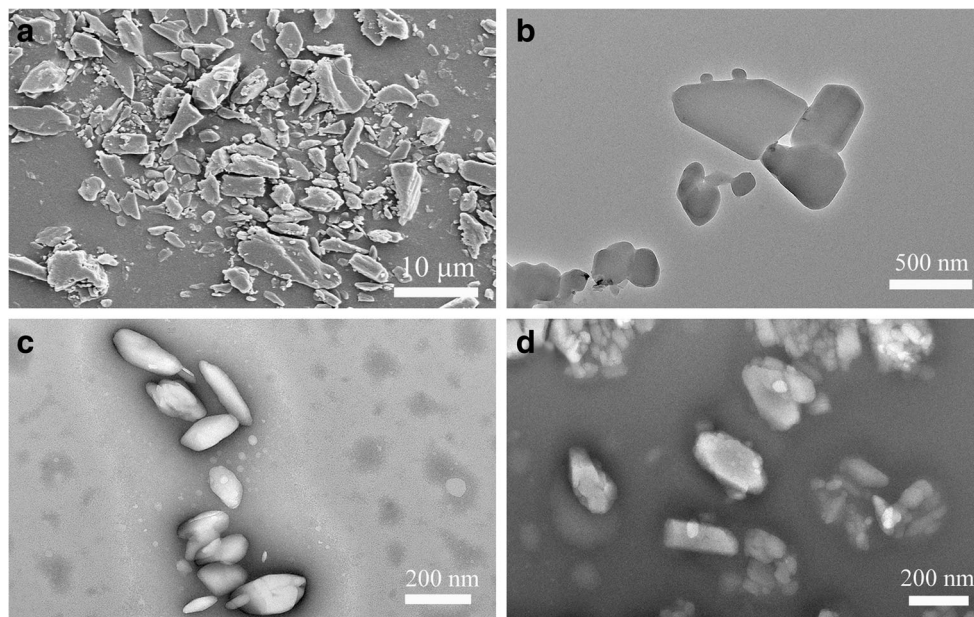
To elucidate the effects of nanosizing processes on drug crystal properties, the solid state of microcrystals, freeze-dried nanocrystals, and the physical mixture was investigated using DSC, PXRD, FT-IR, and Raman spectroscopy, with the results shown below:

DSC

In Fig. 2, the thermal behavior of coarse glyburide, microcrystals, nanocrystals, a physical mixture and an excipient mixture, are reported. First, the DSC thermogram of coarse glyburide (Fig. 2a) presented a sharp peak at 166.8 °C (onset temperature), while the thermal behavior of freeze-dried nanocrystals slightly shifted to a lower temperature. Second, the endothermic peak of nanocrystals (Fig. 2c, d, e) showed an onset temperature at 164.91 °C (Nano-3), 159.65 °C (Nano-

2), and 158.64 °C (Nano-1). The endothermic peak of excipient also was observed in Fig. 2. Third, there was slight and broader shift in the endothermic peak of nanocrystals toward lower temperatures, compared with the peak of the corresponding pure drug, which could be the result of nanonization [21, 22]. The slight shift observed towards lower temperatures might be due to loss of crystallinity and the appearance of the excipients. The H_f decreased from 62.809 J/g (coarse glyburide) up to 30.745 J/g (Nano-3), 20.29 J/g (Nano-2), and 13.35 J/g (Nano-1), further confirming the loss in crystallinity during the milling process. Reduction of the particle size from micro range to the nano range leads to a significant increase in the surface-volume ratio, and a resulting change in surface energy which we anticipated could further affect the intrinsic properties of the drug particles. Weakened thermal resistance and intermolecular interactions in the nanocrystals means that less energy is required to rupture the bonds between the drug molecules [23]. The reflected DSC thermograms exhibited left and broadened peaks, which is most likely due to the size effect and crystal defects during the milling process [24, 25].

Fig. 1 The SEM image of a micronized glyburide, and the TEM images of nanocrystals: **b** Nano-3, **c** Nano-2, and **d** Nano-1. (Nano-3: 601.3 nm; Nano-2: 312.5 nm; Nano-1: 237.6 nm)



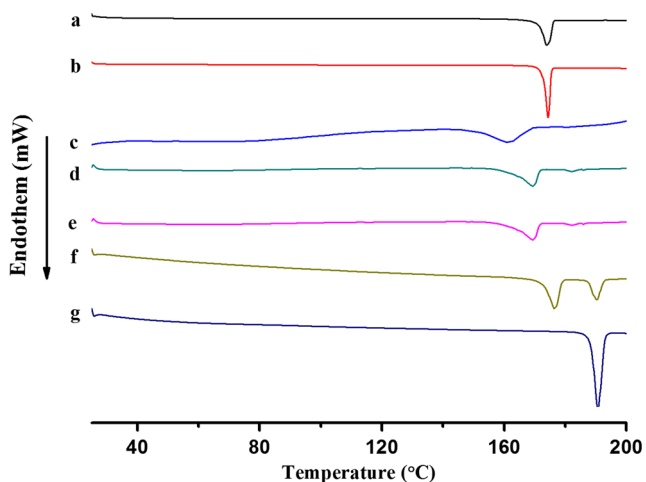


Fig. 2 The DSC thermograms of **a** coarse drug, **b** micronized glyburide, **c** Nano-1, **d** Nano-2, **e** Nano-3, **f** physical mixture, and **g** excipient mixture

PXRD

The PXRD images provided further evidence for the physical state of the glyburide nanocrystals. The diffractogram patterns of coarse glyburide, microcrystals, nanocrystals, the physical mixture, and excipient mixture are presented in Fig. 3. A sharp and intense diffraction peak of coarse glyburide (Fig. 3a) confirms a crystalline nature which is in good agreement with the study by Pei T. Mah and Timo Laaksonen [26]. Characteristic peaks were observed at 2θ of 11.7° , 13.1° , 18.9° , 19.4° , 20.7° , 21.8° , 22.8° , 23.1° , 24.7° , and 25.2° in the untreated glyburide [26]. The reduced intensity and slight broadening of the peaks following nanonization could be due to small drug crystals [24] and the surface coating of the stabilizers [27]. The broad

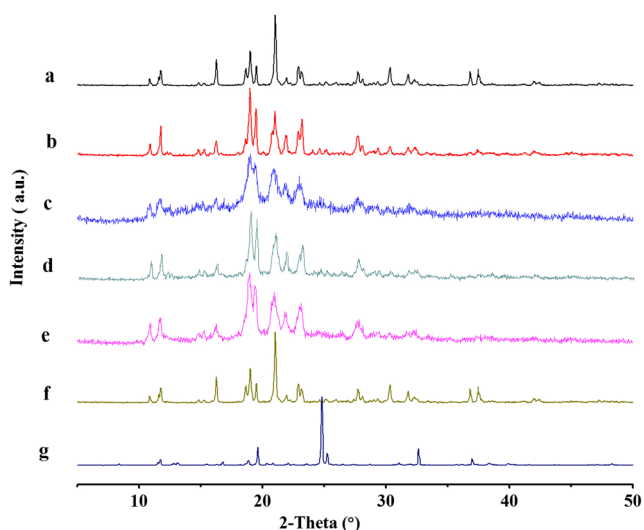


Fig. 3 The X-ray diffraction results of **a** coarse drug, **b** micronized glyburide, **c** Nano-1, **d** Nano-2, **e** Nano-3, **f** physical mixture, and **g** excipient mixture

halo characteristic observed in (Fig. 3b, c, d, e) may attribute to the so-called “size broadening phenomenon” of crystalline materials with sizes less than $1\ \mu\text{m}$ and is related to microstructure changes (crystal size, defects, and microstrain). During milling, collision and shear forces determine the breakdown of the drug crystals from micro range down to the nano range. These high energy forces may also induce a change in crystal structure and partial or total amorphization of the samples [28–30].

FT-IR

Since FT-IR spectroscopy is sensitive to structural changes occurring in a sample, we analyzed the infrared characteristics of the glyburide crystal during the size reduction process and the results obtained are shown in Fig. 4. The main absorption bands of glyburide (Fig. 4a) were observed at 3374.82 , 3319.86 , and $1717.30\ \text{cm}^{-1}$ which corresponded to NH, HN-C=O, and =C-O-C groups, respectively. Sharp peaks at 1306.54 , $1341.25\ \text{cm}^{-1}$ and peaks at 1157.08 , $1183.11\ \text{cm}^{-1}$ are associated with the asymmetric and symmetric stretching vibration of SO_2 . The excipient peaks at 1121 and $1670\ \text{cm}^{-1}$ correspond to C-N and C=O stretching. It was evident from the spectrum that a reduction in band intensity and the loss of spectral resolution occurs upon milling. Both effects are attributable to the nanosizing and drug amorphization process. Moreover, several distinct differences were observed between nanocrystals and microcrystals. First of all, the N-H stretching detected at $3319.86\ \text{cm}^{-1}$ in the coarse glyburide (Fig. 4a) found to mostly disappear in Nano-1, while the N-H stretch at $3374.82\ \text{cm}^{-1}$ remains mostly unchanged. The next obvious difference is that a significant loss of peak intensity was observed at the $1717.30\ \text{cm}^{-1}$ (carbonyl stretching region) of the spectrum of the quenched sample. Apart from the decrease, a

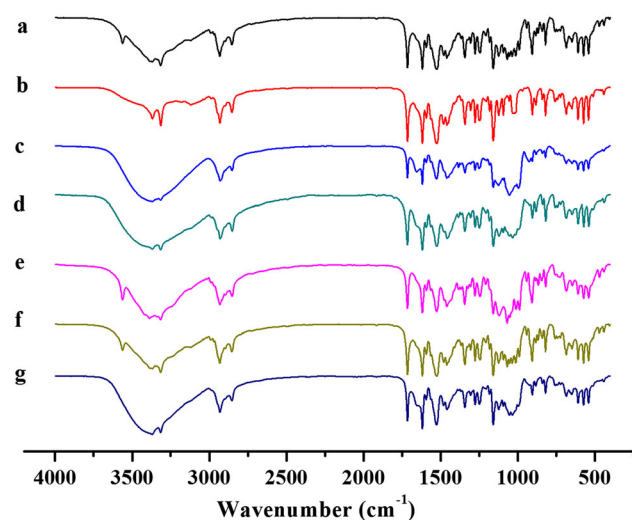


Fig. 4 FT-IR spectra of **a** coarse drug, **b** micronized glyburide, **c** Nano-1, **d** Nano-2, **e** Nano-3, **f** physical mixture, and **g** excipient mixture

new band at 1654 cm^{-1} was found to appear. According to reports in the literature, this new band is attributable to C=N stretching. Also, the spectral changes were connected with the transition between the keto form and the enol form (keto-enol tautomerism) of glyburide, a result of the amide-imidic acid conversion during the milling process [31].

Raman spectroscopy

Raman spectroscopy is a technique which involves examination at the molecular level, and it uses inter- and intramolecular vibrations to investigate structural differences [32]. The Raman spectra of coarse glyburide, microcrystals, and nanocrystals are shown in Fig. 5. Characteristic peaks were observed at 1588 cm^{-1} (C=C stretching), double peaks at 1368 cm^{-1} (asymmetric stretching of SO_2) and 1152 cm^{-1} (symmetric stretching of SO_2), which broadened upon milling. Nanosizing resulted in merging of multiple from 1428 to 1459 cm^{-1} , which could be assigned to a deformation of alkyl groups' vibrations. Furthermore, milling of glyburide resulted in clear reductions in peak intensity at $1014, 1151, 1178, 1199,$ and 1246 cm^{-1} , and the peak is broadening at 1250 cm^{-1} . Often, peak broadening and intensity reduction are related to crystal disorder which was evident in the size reduction process [29].

Equilibrium solubility of glyburide

For solubility measurements, equilibrium solubility methods are preferred to kinetic solubility measurement [33]. The equilibrium solubility of microcrystals and nanocrystals are shown in Fig. 6. The solubility of microcrystals, Nano-2 and Nano-3, was less than 0.4 g/mL for 72 h, and it was clear that Nano-1 exhibited a marked improvement in solubility (from 0.23 to

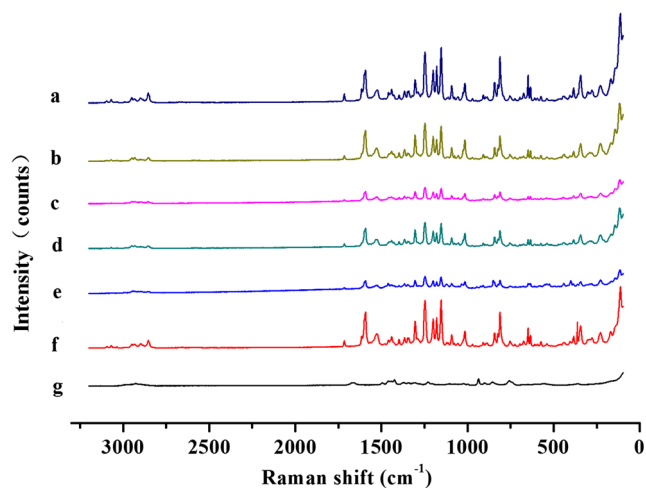


Fig. 5 Raman spectra of **a** coarse drug, **b** micronized glyburide, **c** Nano-1, **d** Nano-2, **e** Nano-3, **f** physical mixture, and **g** excipient mixture

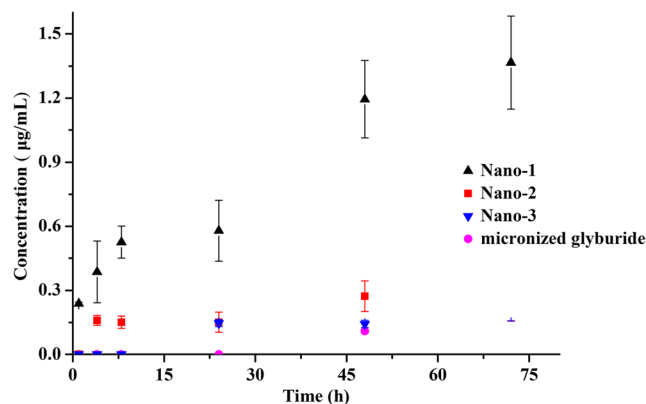


Fig. 6 Equilibrium solubility of micronized glyburide and Nano-3, Nano-2, and Nano-1 in distilled water

$1.36\text{ }\mu\text{g/mL}$). There was no significant increase in solubility between 48 and 72 h ($p > 0.05$), indicating that equilibrium attainment. The poor wettability of the microcrystals powder may partly account for the low solubility of the microcrystals [34] since some of the powder was floating on the medium during the entire shaking process. Following a further reduction, the solubility of Nano-3 and Nano-2 did not show any significant improvement, and this can be explained by the broader size distribution. Differences in the diffusion layer and surface area in nanocrystals are responsible for creating differences in solubility [15]. The research of Bernard Van Eerdenbrugh has suggested that the influence of particle size on the relative solubility (relative to that of the unmilled drug) might only become significant when the particle size is smaller than 300 nm , consistent with our results [35]. The Kelvin and Noyes-Whitney equation could explain the subsequent increase in solubility: A decrease in particle size to 237.6 nm leads to a significant increase in the surface area, which may further reduce the diffusion layer and increase the dissolution pressure, thereby, increasing the solubility. Molecules from highly concentrated solution around small-sized nanocrystals

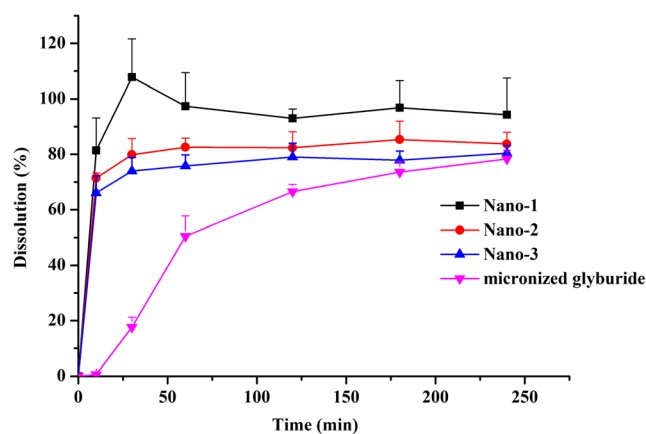


Fig. 7 Dissolution profiles of micronized glyburide and Nano-3, Nano-2, and Nano-1 in pH 6.8 buffer solution containing 0.3% SDS. Each bar represents mean \pm S.E. of three independent experiments

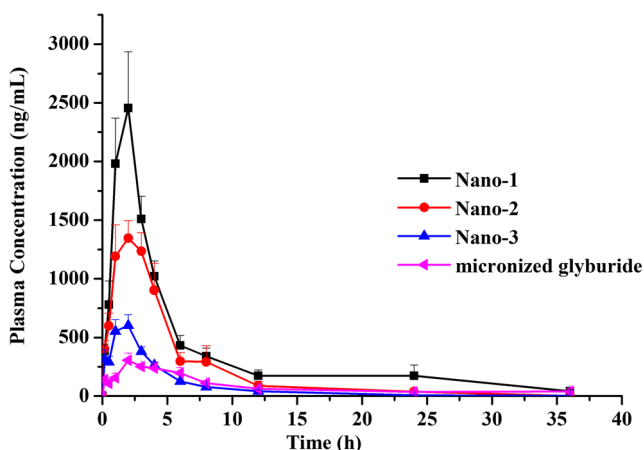


Fig. 8 In vivo plasma concentration of glyburide versus time curves after oral administration of 10 mg glyburide to SD rats (data are mean \pm S.E., $n = 6$)

tend to diffuse into the vicinity of larger nanocrystals where a low concentration is present. This continuous process tends to create a concentration gradient, leading to the dissolution of small crystalline particles and the growth of larger particles as explained by Ostwald ripening [36].

In vitro dissolution performance

The in vitro, dissolution performances of microcrystals and freeze-dried nanocrystals were investigated in a buffer solution of pH 6.8, containing 0.3% SDS. The dissolution profiles are shown in Fig. 7. It is noticeable that glyburide displayed definite improvement after nanosizing. In the case of jet-milled microcrystals, more than 70% of the glyburide dissolved within 4 h; while, nearly 70% of the nanocrystals dissolved within 30 min, as opposed to the only 20% solvation observed with the microcrystals. After 4 h, 100% of the glyburide had dissolved from Nano-1, and Nano-2, preparations, while only about 83.7% dissolved from Nano-3. The dissolution rate was shown to be linearly proportional to the specific surface area, as described by the Noyes–Whitney equation, and it is apparent that the dissolution rate and extent

of dissolution were improved proportionally by breaking drug crystals down to the nano range [28]. Moreover, the dramatic increase in the dissolution rate can result from the enhanced surface area of the reduced particles and the decreased diffusion layer thickness. Overall, fast and complete dissolution was obtained when the particle size was reduced to 237.6 nm. We assumed that this increase in the in vitro dissolution rate would favor in vivo bioavailability.

In vivo bioavailability performance

The plasma drug concentration–time curves of glyburide microcrystals and nanocrystals after oral administration to SD rats are presented in Fig. 8, and the key pharmacokinetic parameters are shown in Table 3. The $AUC_{(0-t)}$ of nanocrystals exhibited a significant increase, compared with the microcrystals. Also, the differences in the pharmacokinetic parameters of the particle sizes were observed and shown to be statistically significant. The $AUC_{(0-36\text{ h})}$ value of Nano-3, Nano-2, and Nano-1 was increased about 2.32-fold ($p < 0.05$), 2.30-fold ($p < 0.05$), and 4.34-fold ($p < 0.01$) compared with microcrystals, respectively. These results clearly proved the effect of nanosizing on the in vivo oral absorption and the necessity of nanosizing. By comparing the pharmacokinetic outcome of microcrystals and nanocrystals, an interesting phenomenon was discovered that the C_{\max} and $AUC_{(0-36\text{ h})}$ showed no improvement when the particle size was reduced from 601.3 to 312.5 nm. As shown in Fig. 8, the time of maximal plasma concentration was achieved later in Nano-3 than in Nano-2, which is indicative of a delayed absorption process. Meanwhile, the $t_{1/2}$ (h) improved from 3.7 to 5.2, and the MRT (h) decreased from 5.2 to 4.9. These results indicated that nanosizing could slow down the elimination of glyburide and sustained the drug in the body for a longer time. When drug nanocrystals are orally administered, they are rapidly dissolved and reach equilibrium solubility in the GI tract. The complete dissolution of the drug, however, is still limited by its solubility within the GI tract. Additionally, it is also reported that particles smaller than 211 nm could penetrate

Table 3 Pharmacokinetic parameters of glyburide formulations after oral administration of a single dose of 10 mg/kg to SD rats, data are presented as mean \pm SE, $n = 6$

Pharmacokinetic parameters	Micronized glyburide	Nano-3	Nano-2	Nano-1
C_{\max} (ng mL ⁻¹)	343.9 \pm 47.4	1760.4 \pm 257.1 ^{###}	1760.4 \pm 257.1	2705.1 \pm 492.3 ^{★★}
T max (h)	3.2 \pm 0.4	2 \pm 0.5	2.0 \pm 0.2	2.0 \pm 0.3
$t_{1/2}$ (h)	13.3 \pm 6.6	3.7 \pm 0.7 ^{###}	5.2 \pm 0.8	6.9 \pm 1.7
$AUC_{(0-36\text{ h})}$ (ng mL ⁻¹ h)	2976.6 \pm 491.1	6895.0 \pm 367.1 ^{##}	6857.8 \pm 369.3	12,928.3 \pm 1591.4 ^{★★★}
MRT (h)	9.9 \pm 1.7	5.2 \pm 0.5	4.9 \pm 0.4	7.7 \pm 1.5

$p < 0.05$ (★), $p < 0.01$ (★★), and $p < 0.001$ (★★★) versus Nano-2 as the control

$p < 0.05$ (*) and $p < 0.01$ (**) versus Nano-3 as the control

$p < 0.05$ (#) and $p < 0.001$ (###) versus microcrystals as the control

to a depth of 60 μm into the gastrointestinal mucous gel layer in rats and retarded the elimination process [37]. Further, it was evident from our findings that, the $t_{1/2}$ of absorption displayed in the micronized glyburide was higher ($p < 0.05$) than the $t_{1/2}$ exhibited in the coarse glyburide. This prolonged period of drug metabolism might be due to the absence of a stabilizer. In fact, when drug crystals are orally administered initially, the undissolved drugs are likely to adhere to the gastrointestinal mucous gel layer, leading to a higher local concentration. After micronization, poor wettability and an increased tendency for electrostatic interaction to occur, make the drug powder more likely to gather in the GI tract, and thus, retard its metabolism [38]. Finally, there was a change in the crystal state from stable microcrystal form to a metastable nanocrystals state [39]. Since the gastrointestinal tract contains gastric fluid, a drug with a high aqueous solubility property is expected to dissolve rapidly [40]. Firstly, particle size affects the dissolution rate of drug crystals; nanocrystals with smaller particle size are supposed to have higher solubility in the GI tract, dissolving faster, whereas larger particles dissolve more slowly. The uptake of dissolved drug crystals can occur via macropinocytosis, caveolin-mediated endocytosis and the M cells in Peyer's patches [14]. Secondly, size-dependent uptake of nanoparticles has also been observed, with nanoparticles of smaller sizes (336.3 nm) demonstrating higher levels of intestinal transport via enterocytes and M cells [41]. Furthermore, particle size affects the penetration through biomembranes of nanocrystals. For example, nanocrystals of fluorescein diacetate can penetrate into the cornea, whereas microcrystals cannot [42]. Compared with coarse hybrid nanocrystals, smaller saquinavir hybrid nanocrystals are more likely internalized by caco-2 cells and translocated into enterocytes and jejunum in vitro [43].

Conclusion

Our present study has clearly demonstrated changes in properties of crystals in the nanosizing procedures. During the milling process, nanocrystals exhibited loss of crystallinity, amide-imidic acid conversion, and partial amorphization. When the particle size reduced to 237.6 nm, the nanocrystals improved in their aqueous solubility properties and in dissolution tests. In the in vivo analysis, reduction of particle size from 601.3 to 312.5 nm showed no improvement in bioavailability, but elimination slowed down moderately, with this reduction. Interestingly, a particle size reduction ranging from 312.5 to 237.6 nm resulted in substantial improvement in both absorption and elimination rates ($p < 0.001$); there was a significant difference in the AUC for nanocrystals, and the ability of the drug to sustain in the rat system for a much longer time. Collectively, our results show that, the reduction of glyburide particle size to 237.6 nm significantly improved the in vitro

and in vivo characteristics, which certainly could favor the therapeutic efficacy of the drug in T2D therapy.

Acknowledgements This work was financially supported by the National Nature Science Foundation for Fostering Talents in Basic Science (J1103606), National Nature Science Foundation of China (No. 81502993), by the Doctoral Research Funding of Liaoning Province (No. 20141066), by the General Project in Education Department of Liaoning Province (No. L2014379), and by the Scientific Research Foundation (QNJJ2013504) and Career Development Program for Young Teachers in Shenyang Pharmaceutical University.

Compliance with ethical standards

Conflicts of interest The authors declare that they have no conflict of interest.

Animal studies All national and institutional guidelines for the care and use of laboratory animals were followed.

References

- Cooper ER. Nanoparticles: a personal experience for formulating poorly water soluble drugs. *Journal of controlled release : official journal of the Controlled Release Society*. 2010;141(3):300–2. doi:10.1016/j.jconrel.2009.10.006.
- Gao L, Liu G, Ma J, Wang X, Zhou L, Li X. Drug nanocrystals: in vivo performances. *Journal of controlled release : official journal of the Controlled Release Society*. 2012;160(3):418–30. doi:10.1016/j.jconrel.2012.03.013.
- Kesisoglou F, Panmai S, Wu Y. Nanosizing—oral formulation development and biopharmaceutical evaluation. *Adv Drug Deliv Rev*. 2007;59(7):631–44. doi:10.1016/j.addr.2007.05.003.
- Khadka P, Ro J, Kim H, Kim I, Kim JT, Kim H, et al. Pharmaceutical particle technologies: an approach to improve drug solubility, dissolution and bioavailability. *Asian Journal of Pharmaceutical Sciences*. 2014;9(6):304–16. doi:10.1016/j.ajps.2014.05.005.
- Sigfridsson K, Lundqvist AJ, Strimfors M. Particle size reduction and pharmacokinetic evaluation of a poorly soluble acid and a poorly soluble base during early development. *Drug Dev Ind Pharm*. 2011;37(3):243–51. doi:10.3109/03639045.2010.505927.
- Eslami F, Elliott JA. Role of precipitating solute curvature on microdrops and nanodrops during concentrating processes: the Nonideal Ostwald-Freundlich equation. *J Phys Chem B*. 2014;118(50):14675–86. doi:10.1021/jp5063786.
- Hattori Y, Haruna Y, Otsuka M. Dissolution process analysis using model-free Noyes-Whitney integral equation. *Colloids Surf B: Biointerfaces*. 2013;102:227–31. doi:10.1016/j.colsurfb.2012.08.017.
- Merisko-Liversidge E, Liversidge GG. Nanosizing for oral and parenteral drug delivery: a perspective on formulating poorly-water soluble compounds using wet media milling technology. *Adv Drug Deliv Rev*. 2011;63(6):427–40. doi:10.1016/j.addr.2010.12.007.
- Godec A, Gaberšček M, Jamnik J. Comment on the Article “A New Understanding of the Relationship between Solubility and Particle Size” by W. Wu and G.H. Nancollas. *J Solut Chem*. 2008;38(1):135–46. doi:10.1007/s10953-008-9354-3.
- Guo Y, Wang Y, Xu L. Enhanced bioavailability of rebamipide nanocrystal tablets: formulation and in vitro/in vivo evaluation.

- Asian Journal of Pharmaceutical Sciences. 2015;10(3):223–9. doi:10.1016/j.ajps.2014.09.006.
11. van Hoogevest P, Liu X, Fahr A. Drug delivery strategies for poorly water-soluble drugs: the industrial perspective. *Expert opinion on drug delivery*. 2011;8(11):1481–500. doi:10.1517/17425247.2011.614228.
 12. Heng JY, Thielmann F, Williams DR. The effects of milling on the surface properties of form I paracetamol crystals. *Pharm Res*. 2006;23(8):1918–27. doi:10.1007/s11095-006-9042-1.
 13. George M, Ghosh I. Identifying the correlation between drug/stabilizer properties and critical quality attributes (CQAs) of nanosuspension formulation prepared by wet media milling technology. *European journal of pharmaceutical sciences : official journal of the European Federation for Pharmaceutical Sciences*. 2013;48(1–2):142–52. doi:10.1016/j.ejps.2012.10.004.
 14. Fu Q, Sun J, Ai X, Zhang P, Li M, Wang Y, et al. Nimodipine nanocrystals for oral bioavailability improvement: role of mesenteric lymph transport in the oral absorption. *Int J Pharm*. 2013;448(1):290–7. doi:10.1016/j.ijpharm.2013.01.065.
 15. Ghosh I, Schenck D, Bose S, Ruegger C. Optimization of formulation and process parameters for the production of nanosuspension by wet media milling technique: effect of vitamin E TPGS and nanocrystal particle size on oral absorption. *European journal of pharmaceutical sciences : official journal of the European Federation for Pharmaceutical Sciences*. 2012;47(4):718–28. doi:10.1016/j.ejps.2012.08.011.
 16. Guo M, Fu Q, Wu C, Guo Z, Li M, Sun J, et al. Rod shaped nanocrystals exhibit superior in vitro dissolution and in vivo bioavailability over spherical like nanocrystals: a case study of lovastatin. *Colloids Surf B: Biointerfaces*. 2015;128:410–8. doi:10.1016/j.colsurfb.2015.02.039.
 17. Fu Q, Sun J, Zhang D, Li M, Wang Y, Ling G, et al. Nimodipine nanocrystals for oral bioavailability improvement: preparation, characterization and pharmacokinetic studies. *Colloids Surf B: Biointerfaces*. 2013;109:161–6. doi:10.1016/j.colsurfb.2013.01.066.
 18. Kasim NA, Whitehouse M, Ramachandran C, Bermejo M, Lennernäs H, Hussain AS, et al. Molecular properties of WHO essential drugs and provisional biopharmaceutical classification. *Mol Pharm*. 2004;1(1):85–96. doi:10.1021/mp034006h.
 19. Cirri M, Righi MF, Maestrelli F, Mura P, Valleri M. Development of glyburide fast-dissolving tablets based on the combined use of cyclodextrins and polymers. *Drug Dev Ind Pharm*. 2009;35(1):73–82. doi:10.1080/03639040802192798.
 20. Li N, Deng Y, Wang D, Qiao Y, Li F. Determination of glibenclamide and puerarin in rat plasma by UPLC-MS/MS: application to their pharmacokinetic interaction study. *Talanta*. 2013;104:109–15. doi:10.1016/j.talanta.2012.11.037.
 21. Shelar DB, Pawar SK, Vavia PR. Fabrication of isradipine nanosuspension by anti-solvent microprecipitation-high-pressure homogenization method for enhancing dissolution rate and oral bioavailability. *Drug delivery and translational research*. 2013;3(5):384–91. doi:10.1007/s13346-012-0081-3.
 22. Zhang D, Tan T, Gao L, Zhao W, Wang P. Preparation of azithromycin nanosuspensions by high pressure homogenization and its physicochemical characteristics studies. *Drug Dev Ind Pharm*. 2007;33(5):569–75. doi:10.1080/03639040600975147.
 23. Ng WK, Kwek JW, Yuen A, Tan CL, Tan R. Effect of milling on DSC thermogram of excipient adipic acid. *AAPS PharmSciTech*. 2010;11(1):159–67. doi:10.1208/s12249-009-9372-5.
 24. Barzegar-Jalali M, Valizadeh H, Shadbad M-RS, Adibkia K, Mohammadi G, Farahani A, et al. Cogrounding as an approach to enhance dissolution rate of a poorly water-soluble drug (gliclazide). *Powder Technol*. 2010;197(3):150–8. doi:10.1016/j.powtec.2009.09.008.
 25. Singh SK, Prasad Verma PR, Razdan B. Glibenclamide-loaded self-nanoemulsifying drug delivery system: development and characterization. *Drug Dev Ind Pharm*. 2010;36(8):933–45. doi:10.3109/03639040903585143.
 26. Mah PT, Laaksonen T, Rades T, Peltonen L, Strachan CJ. Differential scanning calorimetry predicts the critical quality attributes of amorphous glibenclamide. *European journal of pharmaceutical sciences : official journal of the European Federation for Pharmaceutical Sciences*. 2015;80:74–81. doi:10.1016/j.ejps.2015.08.006.
 27. Hecq J, Deleers M, Fanara D, Vranckx H, Amighi K. Preparation and characterization of nanocrystals for solubility and dissolution rate enhancement of nifedipine. *Int J Pharm*. 2005;299(1–2):167–77. doi:10.1016/j.ijpharm.2005.05.014.
 28. Jinno J, Kamada N, Miyake M, Yamada K, Mukai T, Odomi M, et al. Effect of particle size reduction on dissolution and oral absorption of a poorly water-soluble drug, cilostazol, in beagle dogs. *Journal of controlled release : official journal of the Controlled Release Society*. 2006;111(1–2):56–64. doi:10.1016/j.jconrel.2005.11.013.
 29. Mah PT, Laaksonen T, Rades T, Aaltonen J, Peltonen L, Strachan CJ. Unravelling the relationship between degree of disorder and the dissolution behavior of milled glibenclamide. *Mol Pharm*. 2014;11(1):234–42. doi:10.1021/mp4004145.
 30. Deng Z, Xu S, Li S. Understanding a relaxation behavior in a nanoparticle suspension for drug delivery applications. *Int J Pharm*. 2008;351(1–2):236–43. doi:10.1016/j.ijpharm.2007.10.001.
 31. Wojnarowska Z, Grzybowska K, Adrjanowicz K, Kaminski K, Paluch M, Hawelek L, et al. Study of the amorphous glibenclamide drug: analysis of the molecular dynamics of quenched and cryomilled material. *Mol Pharm*. 2010;7(5):1692–707. doi:10.1021/mp100077c.
 32. Nanubolu JB, Burley JC. Investigating the recrystallization behavior of amorphous Paracetamol by variable temperature Raman studies and surface Raman mapping. *Mol Pharm*. 2012;9(6):1544–58. doi:10.1021/mp300035g.
 33. Dressman JB, Vertzoni M, Goumas K, Reppas C. Estimating drug solubility in the gastrointestinal tract. *Adv Drug Deliv Rev*. 2007;59(7):591–602. doi:10.1016/j.addr.2007.05.009.
 34. Fong SYK, Ibisogly A, Bauer-Brandl A. Solubility enhancement of BCSS Class II drug by solid phospholipid dispersions: spray drying versus freeze-drying. *Int J Pharm*. 2015;496(2):382–91. doi:10.1016/j.ijpharm.2015.10.029.
 35. Van Eerdenbrugh B, Vermant J, Martens JA, Froyen L, Humbeeck JV, Van den Mooter G, et al. Solubility increases associated with crystalline drug nanoparticles: methodologies and significance. *Mol Pharm*. 2010;7(5):1858–70. doi:10.1021/mp100209b.
 36. Vogelsberger W. Thermodynamic and kinetic considerations of the formation and the dissolution of nanoparticles of substances having low solubility. *J Phys Chem B*. 2003;107(36):9669–76. doi:10.1021/jp030347z.
 37. Baek IH, Kim JS, Ha ES, Choo GH, Cho W, Hwang SJ, et al. Dissolution and oral absorption of pranlukast nanosuspensions stabilized by hydroxypropylmethyl cellulose. *Int J Biol Macromol*. 2014;67:53–7. doi:10.1016/j.ijbiomac.2014.03.006.
 38. Scholz A, Abrahamsson B, Diebold SM, Kostewicz E, Polentarutti BI, Ungell A-L, et al. Influence of hydrodynamics and particle size on the absorption of felodipine in labradors. *Pharm Res*. 2002;19(1):42–6. doi:10.1023/A:1013651215061.
 39. Fu Q, Kou L, Gong C, Li M, Sun J, Zhang D, et al. Relationship between dissolution and bioavailability for nimodipine colloidal dispersions: the critical size in improving bioavailability. *Int J Pharm*. 2012;427(2):358–64. doi:10.1016/j.ijpharm.2012.02.022.

40. Pathak K, Raghuvanshi S. Oral bioavailability: issues and solutions via nanoformulations. *Clin Pharmacokinet.* 2015;54(4):325–57. doi:10.1007/s40262-015-0242-x.
41. He C, Yin L, Tang C, Yin C. Size-dependent absorption mechanism of polymeric nanoparticles for oral delivery of protein drugs. *Biomaterials.* 2012;33(33):8569–78. doi:10.1016/j.biomaterials.2012.07.063.
42. Baba K, Tanaka Y, Kubota A, Kasai H, Yokokura S, Nakanishi H, et al. A method for enhancing the ocular penetration of eye drops using nanoparticles of hydrolyzable dye. *Journal of controlled release : official journal of the Controlled Release Society.* 2011;153(3):278–87. doi:10.1016/j.jconrel.2011.04.019.
43. He Y, Xia DN, Li QX, Tao JS, Gan Y, Wang C. Enhancement of cellular uptake, transport and oral absorption of protease inhibitor saquinavir by nanocrystal formulation. *Acta Pharmacol Sin.* 2015;36(9):1151–60. doi:10.1038/aps.2015.53.